Volume 9, Number 12
1009-1963/2000/09(12)/0913-09
CHINESE PHYSICS
December, 2000
© 2000 Chin. Phys. Soc.

RESEARCH ON VIBRATION MODES OF THE CHINESE CHIME STONE*

Cheng Jian-zheng(程建政), Zhang De-jun(张德俊),
Lan Cong-qing(兰从庆), Ye Chao-hui(叶朝辉)
Wuhan Institute of Physics and Mathematics, Chinese Academy of Sciences Wuhan 430071, *China*

(Received 4 June 2000)

Nearfield acoustical holography is a powerful tool for imaging of acoustic sources. In this article, the basic theory treating steady-state acoustic radiation with generalized holography has been discussed. By holographic imaging, the vibration characteristics of irregular objects, the Chinese ancient musical instrument, the one-tone chime stone and the two-tone chime stone provided by the Institute of Archaeology, the Museum of Hubei Province, have been researched. The results show that the ancient chime stone has two main vibration modes, which make up the base of sound produced by the instrument. As for the two-tone chime stone, it is not so long and wide as the single-tone chime stone, but thicker and smoother than the single-tone chime stone. When it is excited at different positions, although it radiates sounds of different frequencies, its vibration modes are similar. This may be related to its dimensions and shape. The research is helpful for studying the sound producing system and the radiated field characteristics of the chime stone.

Keywords: holography, chime stone, vibration mode
PACC: 4363, 4375

I. INTRODUCTION

Nearfield acoustical holography is a new acoustical imaging technique and is developed from the traditional acoustical holography. Since it was first presented by Williams and Maynard,[1−4] many researches have been done in this area.[5−9] In the traditional acoustical holography, the hologram is recorded in the Fresnel region or Fraunhofer region with the distance between the receiving plane and the object plane much greater than the radiated wavelength, therefore, only the propagating wave components can be recorded. According to the Rayleigh criterion, the resolution distance of the traditional acoustical holography cannot be smaller than half wavelength. Different from the traditional acoustical holography, nearfield acoustical holography records the hologram very close to the object plane; it records not only the propagating wave components but also the evanescent wave components, which exponentially decay with propagating distance. Because the evanescent wave components express the details of the object vibration, the reconstructed image can have a resolution better than half wavelength. In addition, the distribution of particle velocity and vector intensity can be calculated simultaneously. Because of the advantage of the nearfield acoustical holography, it can be used to measure and analyze the vibration mode of the source, the strength of the construction, the quality of the adhesion and welding, to locate noise, to trace propagating way of the sound energy. It is especially useful for the source vibration and radiation problems with irregular shapes or complicated boundary conditions, which are very difficult or impossible to calculate theoretically.

Ⅱ. THEORY FOR PLANAR NEARFIELD ACOUSTICAL HOLOGRAPHY

Assume that the object vibrates at a constant frequency. From the wave equation and Green's theorem, given the pressure $\psi(Q_0)$ on an arbitrary surface S, the complex pressure at any point $Q(x,y,z)$ enclosed by S can be written as[10]

$$\psi(Q) = \frac{1}{4}\int_s \left[\frac{\partial\psi(Q_0)}{\partial n}g(Q,Q_0) - \psi(Q_0)\frac{\partial g(Q,Q_0)}{\partial n}\right]\mathrm{d}S, \qquad (1)$$

where g and $\partial g/\partial n$ are the free-space Green's function and its normal derivative respectively. When S is an infinite plane S_p with a hemispherical dome S_d at infinity, the integral on the hemisphere S_d in Eq.(1) can be neglected. If the value of the field on the plane S_p, $\psi(Q_0)$ (the Dirichlet boundary condition) is given and the Green's function is chosen to satisfy $g(Q,Q_0)=0$ on S_p, Eq.(1) becomes

$$\psi(Q) = -\frac{1}{4\pi}\int_s \psi(Q_0)\frac{\partial g(Q,Q_0)}{\partial n}\mathrm{d}S. \qquad (2)$$

*Project supported by the National Natural Science Foundation of China, (Grant No.19634050) and the State key Laboratory of Acoustics.

The Green's function that satisfies the above boundary condition can be expressed as

$$g_-(Q,Q_0)=\frac{e^{jkr}}{r}-\frac{e^{jkr'}}{r'}, \tag{3}$$

where

$$r=\sqrt{(x-x_0)^2+(y-y_0)^2+(z-z_0)^2},$$

$$r'=\sqrt{(x-x_0)^2+(y-y_0)^2+(z+z_0-2z_s)^2},$$

which vanishes on the plane $z_0=z_s$. From Eq.(3), we can see that $g_-(Q,Q_0)$ is the sum of two point sources with opposite phases; one is at point Q and the other at the mirror point of point Q about the plane S_p; (x_0,y_0,z_0) is the Cartesian co-ordinate of any point in space and (x_s,y_s,z_s) is on S_p.

$$\frac{\partial g_-(Q,Q_0)}{\partial n}\Big|_{S_p}=2\frac{(jkr-1)(z-z_s)e^{jkr}}{r^3}.$$

To simplify the notation, we define

$$\begin{aligned}g_D(Q,Q_s)&=-\frac{1}{4\pi}\frac{\partial G_-(Q,Q_0)}{\partial n}\Big|_{S_p}\\&=(z-z_s)(1-jkr)\frac{e^{jkr}}{2\pi r^3}.\end{aligned} \tag{4}$$

Equation (2) becomes

$$\begin{aligned}\psi(x,y,z)=&\int_{-\infty}^{\infty}\int_{-\infty}^{\infty}\psi(x_s,y_s,z_s)\\&\times g_D(x-x_s,y-y_s,z-z_s)\mathrm{d}x_s\mathrm{d}y_s\end{aligned} \tag{5}$$

or

$$\psi(x,y,z)=\psi(x,y,z_s)*g_D(x,y,z-z_s).$$

With the two-dimensional spatial Fourier transform, it can be written as

$$\psi(k_x,k_y,z)=\psi(k_x,k_y,z_s)\cdot G_D(k_x,k_y,z-z_s), \tag{6}$$

where $G_D(k_x,k_y,z)$ can be deduced from the Helmholtz equation $(\nabla^2+k^2)\psi=0$ with the theory of the angular spectrum[11]

$$G_D(k_x,k_y,z)=F[g(x,y,z)]=e^{jz\sqrt{k^2-k_x^2-k_y^2}}. \tag{7}$$

In Eq.(1), if the normal derivative of the field on the plane S_p, $\partial\psi(Q_0)/\partial n$ (the Neuman boundary condition) is given and the Green's function is chosen to satisfy $\partial g(Q,Q_0)/\partial n=0$ on S_p, Eq.(1) becomes

$$\psi(Q)=\frac{1}{4\pi}\int_s g(Q,Q_0)\frac{\partial\psi(Q_0)}{\partial n}\mathrm{d}S. \tag{8}$$

The Green's function that satisfies the above boundary condition can be expressed as

$$g_+(Q,Q_0)=\frac{e^{jkr}}{r}+\frac{e^{jkr'}}{r'}, \tag{9}$$

whose normal derivative vanishes on the plane $z_0=z_s$. From Eq.(3), we can see that $g_+(Q,Q_0)$ is the sum of two point sources with the same phase. We define

$$g_N(Q,Q_s)=\frac{1}{4\pi}g_+(Q,Q_0)\Big|_{S_p}=\frac{e^{jkr}}{2\pi r}, \tag{10}$$

Equation (8) becomes

$$\begin{aligned}\psi(x,y,z)=&\int_{-\infty}^{\infty}\int_{-\infty}^{\infty}\frac{\partial\psi(x_s,y_s,z_s)}{\partial n}\\&g_N(x-x_s,y-y_s,z-z_s)\mathrm{d}x_s\mathrm{d}y_s\end{aligned} \tag{11}$$

or

$$\psi(x,y,z)=\frac{\partial\psi(x,y,z_s)}{\partial n}*g_N(x,y,z-z_s).$$

With the two-dimensional spatial Fourier transform, it can be written as

$$\begin{aligned}\psi(k_x,k_y,z)=&F\left\{\frac{\partial\psi(x_s,y_s,z_s)}{\partial n}\right\}\\&\times G_N(k_x,k_y,z-z_s)\end{aligned} \tag{12}$$

where

$$\begin{aligned}G_N(k_x,k_y,k_z)&=F[g_N(x,y,z)]\\&=\frac{e^{jz\sqrt{k^2-k_x^2-k_y^2}}}{j\sqrt{k^2-k_x^2-k_y^2}}\end{aligned} \tag{13}$$

From the deduction above, if the field or its normal derivative on the source plane is given, the field of arbitrary space point can be obtained. To the contrary, if the field on a certain plane is given, the field and its normal derivative on the source plane can be reconstructed. As we know, the hologram data are usually not measured right on the source plane $z=z_S$, but on a plane $z=z_H$ parallel to the source plane. Evaluating Eq.(6) or Eq.(12) with $z=z_H$ yields

$$\begin{aligned}\psi(k_x,k_y,z_H)=&\psi(k_x,k_y,z_S)\\&\times G_{D,N}(k_x,k_y,z_H-z_S).\end{aligned} \tag{14}$$

Solving Eq.(14) for $\psi(k_x,k_y,z_S)$ and substituting in Eq.(6) or Eq.(12) yields

$$\begin{aligned}\psi(k_x,k_y,z)&=\psi(k_x,k_y,z_H)\cdot\frac{G_{D,N}(k_x,k_y,z-z_S)}{G_{D,N}(k_x,k_y,z_H-z_S)}\\&=\psi(k_x,k_y,z_H)\cdot G_{D,N}(k_x,k_y,z-z_H).\end{aligned} \tag{15}$$

Ⅲ. NOISE AND FILTERING IN RECONSTRUCTION

Because of the exponential amplification to the evanescent wave components in the process of the reconstruction for the source, the small measurement errors will cause great errors in the reconstructed image. Actually, due to the surroundings noise and electronic noise, the measurement errors cannot be avoided. In order to solve this problem, Fleischer[12] used Wiener filtering which needs to know the power spectra of the signal and the noise; Veronesi[4] presented a method using a window function in spatial frequency domain to deal with the errors and the noise. The window function has the form as follows

$$W(k_x,k_y)=\begin{cases}1-\dfrac{e^{(k_r/k_c-1)/\alpha}}{2}, & k_r\le k_c\\ \dfrac{e^{(1-k_r/k_c)/\alpha}}{2}, & k_r>k_c\end{cases} \tag{16}$$

where $k_r^2=d_x^2+k_y^2$, $k_c=0.6\pi/d$, $\alpha=0.2$, d is the sampling interval in the holographic plane.

Equation.(16) is effective when $z-z_H$ is very small, but it will be defective when $z-z_H$ becomes larger. We presented a new filtering method-least square method for filtering with restraint as follows[13]

$$W_d(k_x,k_y)=\begin{cases}\dfrac{1}{1+(\varepsilon/E)^2k_r^2}, & k_r\le k\\ \dfrac{1}{1+(\varepsilon/E)^2k_r^2\exp(2|z-z_H|\sqrt{k_r^2-k^2})}, & k_r>k\end{cases} \tag{17}$$

where ε/E is the SNR. Comparing Eq.(16) with Eq.(17), it is easy to see that the Veronesi's filtering function is related to the sampling interval d, k_x and k_y, while the filtering function $W_d(k_x,k_y)$ we presented is related to ε/E and the measuring distance $|z-z_H|$ in addition to k_x and k_y. The larger the ε/E and $|z-z_H|$, the more effective the filtering function $W_d(k_x,k_y)$. So it can suppress the noise and preserve the evanescent wave components much better than $W(k_x,k_y)$ in bad noise condition and large distance $|z-z_H|$.

Ⅳ. EXPERIMENTAL RESEARCH ON CHINESE CHIME STONE

The chime stone is a kind of beating musical instrument made of stone in ancient China. From the single chime stone in Shang dynasty to a series of chime stones in Zhanguo dynasty, it reflected the prominent achievement of the Chinese people in the ancient musical instrument. The irregular geometry and non-uniform thickness of the chime stone make the theoretical research on its vibration modes very difficult. But the study of its vibration modes is very important for understanding its sound system. With the nature of reconstructing the vibration of the nearfield acoustical holographic image, we have investigated experimentally the vibration and radiation characteristics of the one-tone chime stone and the two-tone chime stone provided by the Institute of Archaeology, the Museum of Hubei Province in our laboratory.

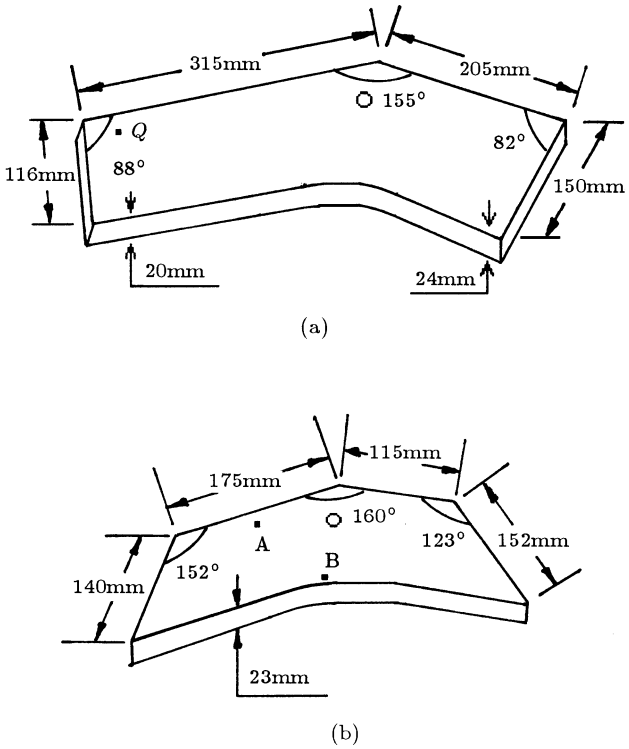


Fig.1. the contour of the Chime stone (a) the Single-tone Chime stone (b) Two-tone chime stone

The contours of the chime stones is shown in Fig.1. The block diagram of experimental system is shown in Fig.2. In the experiment, we hit the beating point of the chime stones, then record the radiated sound signals. By Fourier analysis, we can find out its main frequencies in their spectra. Then we excite the chime stones at the beating point with the vibration exciter at these frequencies respectively. With an array scanning imaging system, the holograms of the different frequencies are recorded in computer, and with the help of the nearfield acoustical holographic imaging, we can reconstruct the vibration modes of the chime stones at different frequencies.

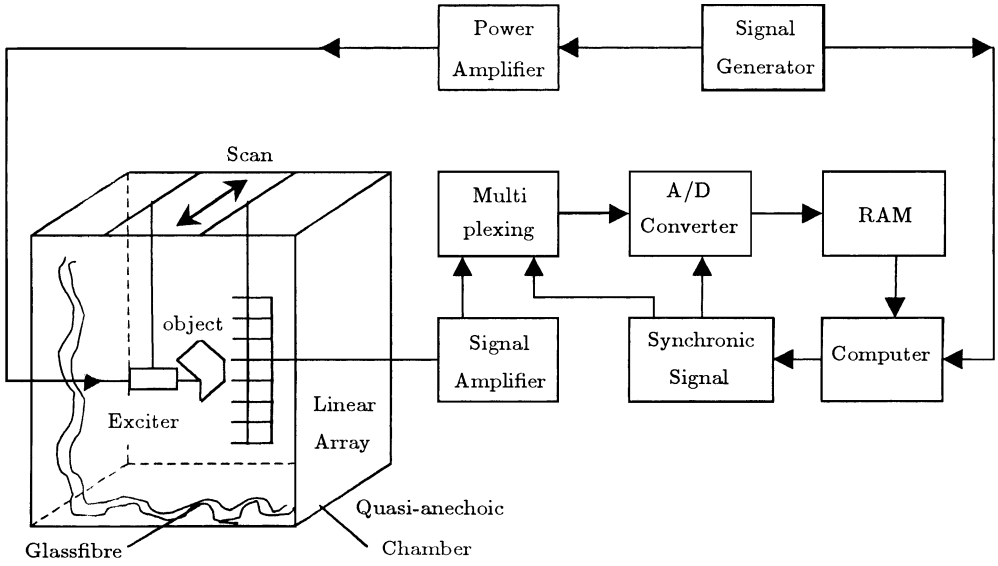
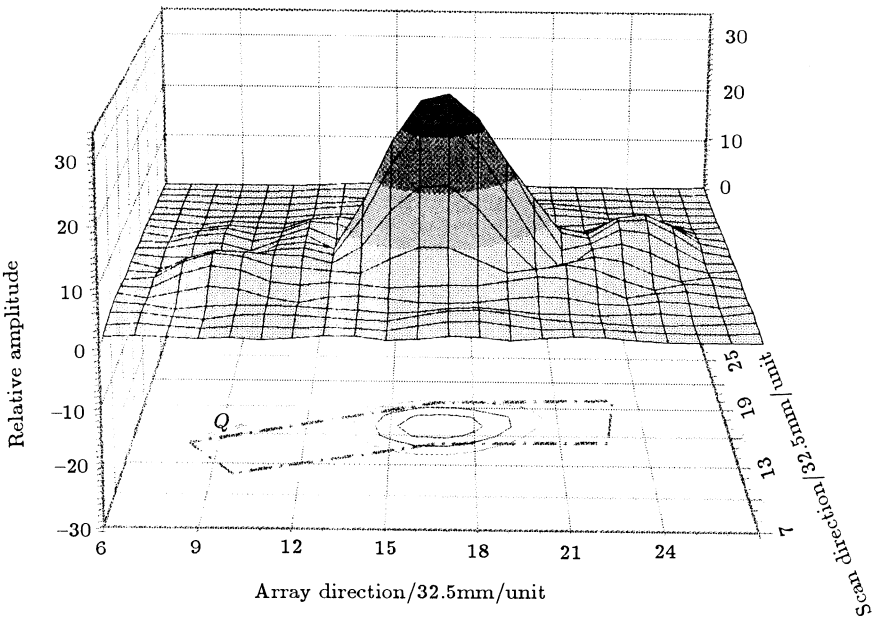


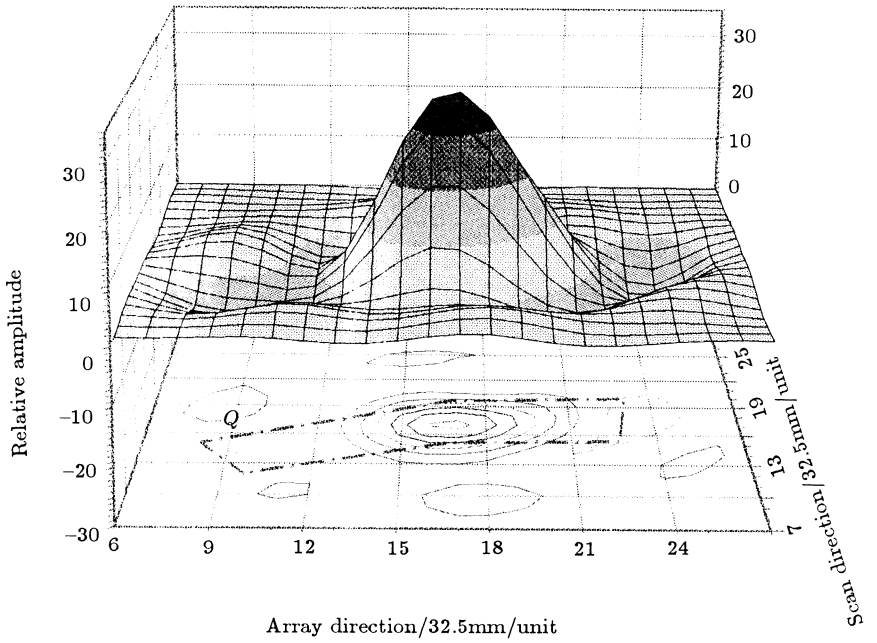
Fig.2. Block diagram of experimental system

A. The single-tone chime stone

A single-tone chime stone has one beating point when being performed. By spectrum analysis, we find that the single-tone chime stone usually has two main vibration frequencies. One is correspondent to the fundamental tone and the other the second harmonic partial. Figure 3 shows the reconstructed fundamental vibration mode of the single-tone chime stone at frequency 450Hz by nearfield acoustical holographic imaging. The dotted line frame indicates the position of the chime stone and the point Q is the beating point. It can be seen that on the fundamental mode, the strongest vibration is on the curved interface of the two parts and the vibration at two poles very weak. The harmonic modes are much more complicated Figure 4 shows the second harmonic vibration pattern at frequency 945Hz. It can be found that the strongest vibration is at the two poles and the vibration in the middle is weak. At the wider side, there an opposite phase vibration, which is twisted to the longitudinal vibration.

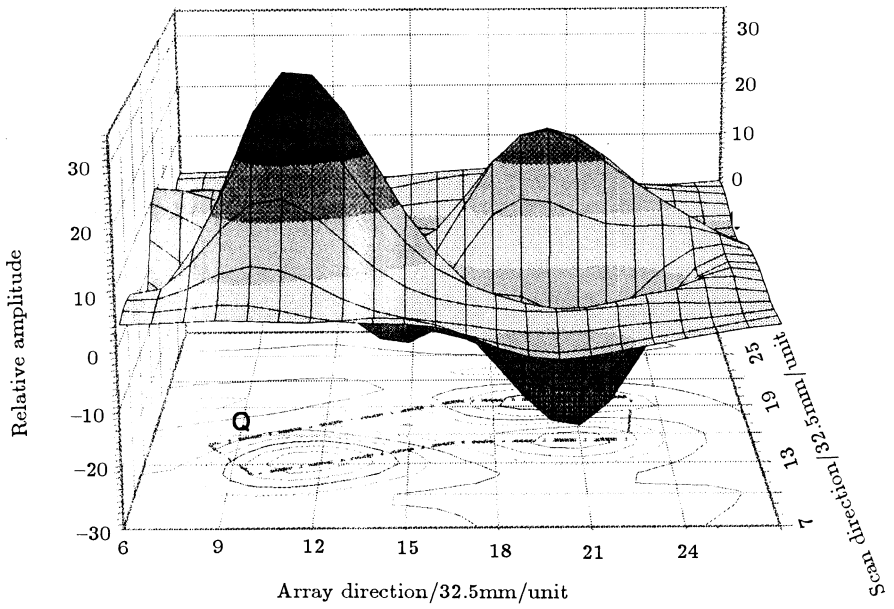


(a)

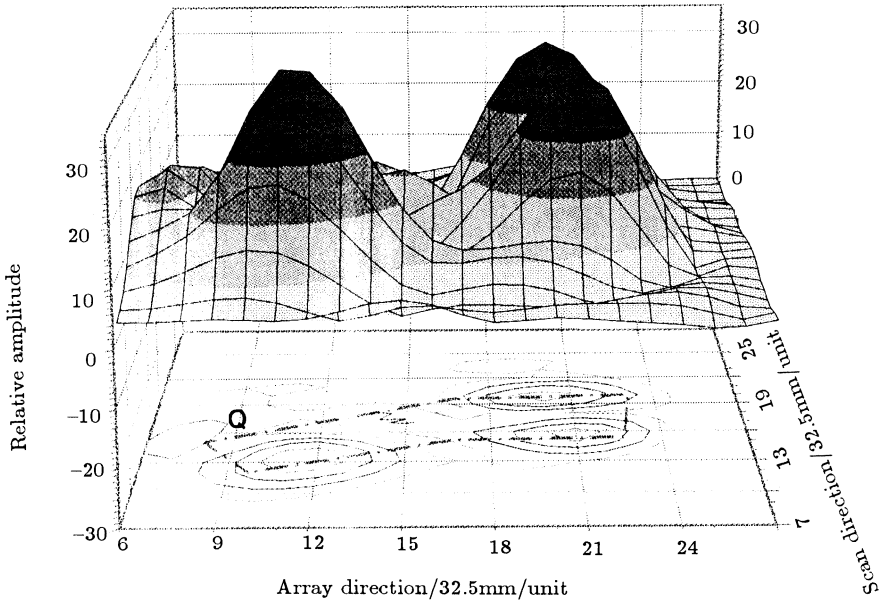


(b)

Fig.3. the reconstructed vibration mode of the single-tone chime stone at frequency 450Hz (a) the amplitude of vibration mode (b) the distribution of instantaneous vibration



(a)

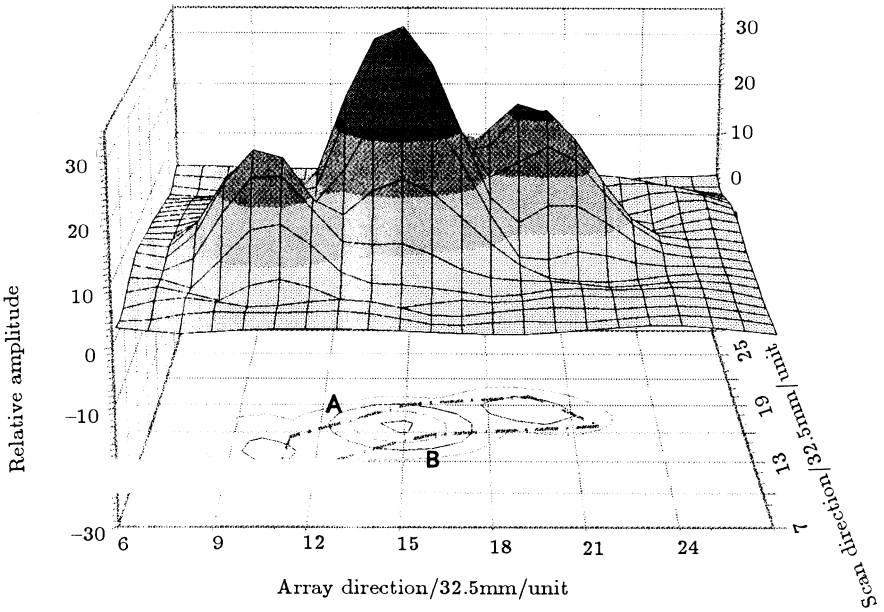


(b)

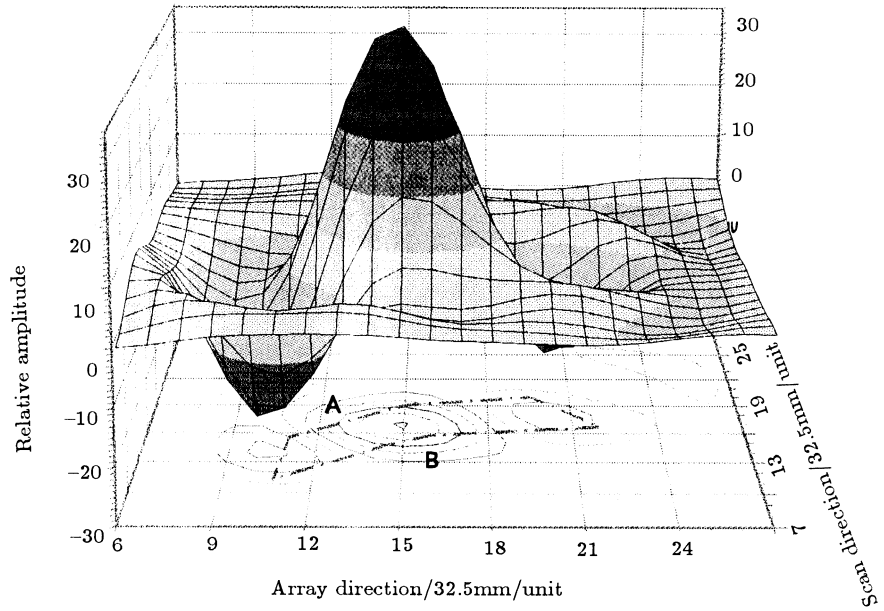
Fig.4. The reconstructed vibration mode of the single-tone chime stone at frequency 945Hz
(a) The amplitude of vibration mode (b) The distribution of instantaneous vibration

B. The two-tone chime stone

A two-tone chime stone has two beating points when being performed. When beaten at the different points, it produces different souns. That is to say, two-tone chime stone has two fundamental frequencies corresponding to two beating points. The two-tone chime stone used in our experiment was made by the Institute of Archaeology, the Museum of Hubei Province. The two beating points are located near the center of the two edges respectively, shown as A and B in Figs.5 and 6, which are the vibration distributions excited at different points with different frequencies. Comparing Fig.5 with Fig.6, we can find that although the excited points and the frequencies of the radiated sound are different, the vibration modes are similar–the vibration in the middle is strong and that at the two



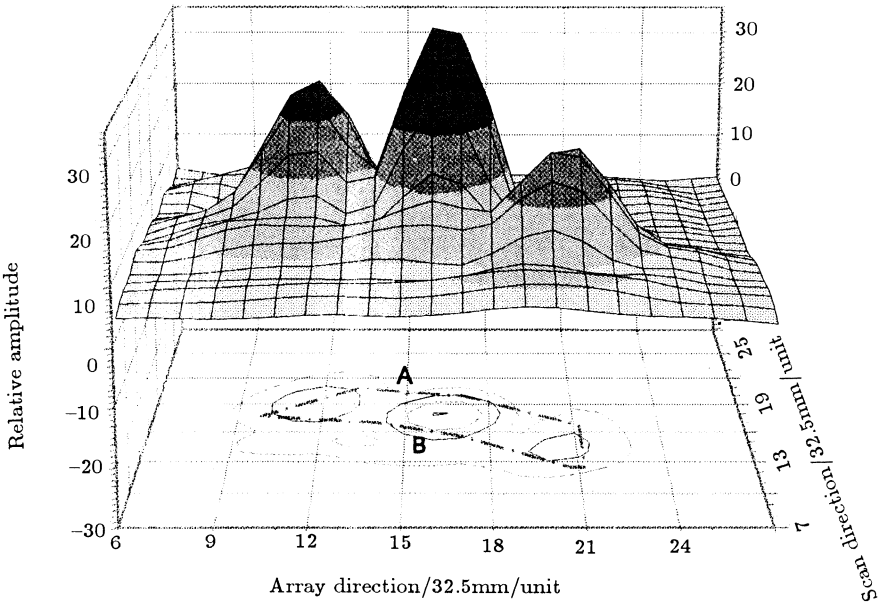
(a)



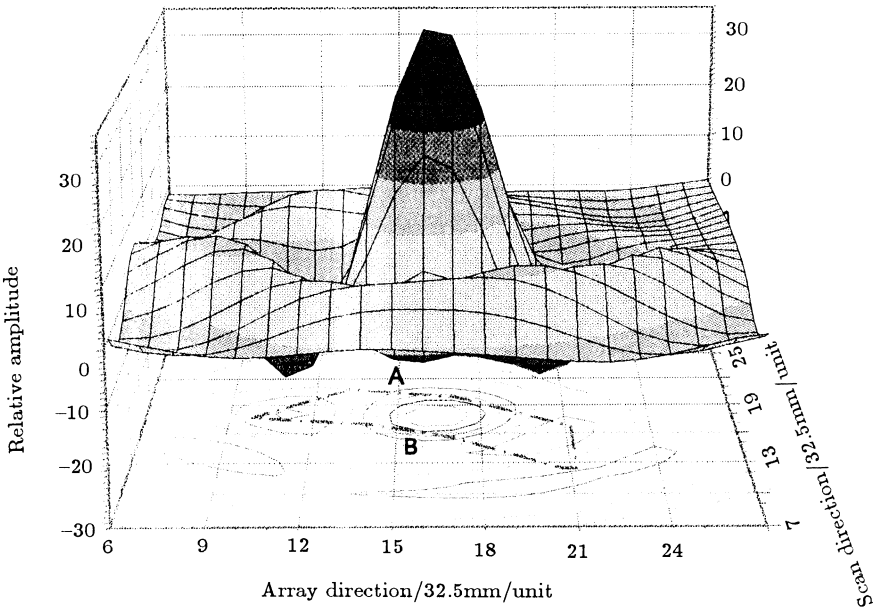
(b)

Fig.5. the reconstructed vibration mode of the two-tone chime stone excited at point A with frequency 1050Hz (a) the amplitude of vibration mode (b) the distribution of instantaneous vibration

poles weaker. There are two node lines in the longitudinal direction, which is similar to (0,2) mode of a rectangle plate. Comparing with the single-tone chime stone, we find that because of its dimension smaller than the of the single-tone chime stone. the fundamental frequencies of its radiated sound are much higher than that of the single-tone chime stone. Because the ratios of its thickness to its length and width are much greater than that of the single-tone chime stone, the high order harmonic partials are hard to be excited. Because the frequencies of radiated sound excited at different points are very close, the vibration modes are similar. But with further investigation we can find that the two vibration modes have different relations with the geometry of the two-tone chime stone. Maybe this is the reason of two tones produced.



(a)



(b)

Fig.6. The reconstructed vibration mode of the two-tone chime stone excited at point B with frequency 960Hz (a) the amplitude of vibration mode (b) the distribution of instantaneous vibration

V. CONCLUSION

With the help of the nearfield acoustical holographic imaging, we have researched on the vibration modes of the irregular objects, the Chinese chime stones, and obtained some meaningful results. First, the chime stone has complicated vibration modes, which are quite different from that of the rectangle plate, and the vibration modes are related with its unique geometrical shape. Second, the harmonic partial mode is more complicated than the fundamental frequency mode. This work is very helpful for explaining the sound producing system of the chime stone. It also provides the scientific basis for designing, making and evaluating of the chime stone. The research also shows that the nearfield acoustical holographic imaging is an effective tool for studying the vibration and radiated field of objects with irregular shapes.

REFERENCES

[1] E. G. Williams and J. D. Maynard, *Phys. Rev. lett.,* **45**(1980),554-557.

[2] E. G. Williams, J. D. Maynard and E. Skudrzyk, *J. Acoust. Soc. Am.,* **68**(1980),340-344.

[3] J. D. Maynard, E. G. Williams and Y. Lee, *J. Acoust. Soc. Am.,***78**(1985),1395-1413.

[4] W. A. Veronesi and J. D. Maynard, *J. Acoust. Soc. Am.,* **81**(1987),1307-1322.

[5] T. Loyan and J. C. Pascal, *J. Acoust. Soc. Am.,* **84** (1988),1744-1750.

[6] E. G. Williams *et al, J. Acoust. Soc. Am.,* **81**(1987),389-407.

[7] G. V. Borgiotti *et al*, *J. Acoust. Soc. Am.,* **88**(1990),199-209.

[8] Angie Sarkission, *J. Acoust. Soc. Am.,* **88**(1990),961-966.

[9] W. A. Veronesi and J. D. Maynard, *J. Acoust. Soc. Am.,* **85**(1989),588-598.

[10] P. M. Morse and K. U. Ingard, Theoretical Acoustics (McGraw-Hill, New York,1968).

[11] J. W. Goodman: Introduction to Fourier Optics (New York, N. K., 1968).

[12] Fleischer H. *et al, Acoustica* **60**(1986),172.

[13] D. J. Zhang *et al, Chinese Journal of Acoustics,* **12** (1993),39-46.